STABILITY RESEARCH ON A NATURAL CIRCULATION DRIVEN SCWR

C. T'Joen, F. Kam and M. Rohde
Delft University of Technology, Delft, The Netherlands

Abstract

To improve the thermal efficiency of nuclear reactors, a concept design using supercritical water has been proposed. As an inherent safety feature, natural circulation could be applied, driving the flow with the strong density changes. Such natural circulation flows can however experience instabilities (density wave oscillations). To study the stability, an experimental facility representing the HPLWR was designed using a scaling fluid (R23). In parallel a computational tool was developed which uses a transient analysis technique. This paper will present a comparison of the experimental measurements and numerical predictions for the stability of a supercritical loop, showing good agreement.

Introduction

As the global energy demand continues to rise rapidly, it is clear that nuclear power will continue to supply an important share of the energy supply in the coming decades, as noted in the projections by the of OECD/IEA (2008) [1]. Currently, nuclear power provides about 16% of the total electricity production worldwide. Nuclear power also offers advantages with respect to environmental protection related to its low CO_2 emissions compared to other power generation means. As such the European Commission recently presented the 'Vision Report of the Sustainable Nuclear Energy Technology Platform' for the European transition towards a low-carbon energy mix by 2050 [2]. The long-term application of nuclear power relies on the development of reactors of generation IV (Gen-IV) with enhanced economics (higher thermal efficiency), minimisation of resource use and waste, and security features. The Gen-IV International Forum (GIF) recommended six innovative nuclear reactor concepts and proposed a technology roadmap [3]. These designs differ significantly, both from the thermo-hydraulic point of view (using a wide range of coolants: liquid metals, supercritical water, helium and molten salts) and from the neutronic point of view (hard, thermal or mixed neutron spectra).

The supercritical water reactor, SCWR, is one of the proposed designs. It is a light water cycle based on supercritical water, and can thus be seen as a logical extension of the evolution of light water reactors by raising the pressure, moving from boiling water reactors (BWR) to pressurized water reactor (PWR). This evolution also took place in fossil fuel fired power plants, leading to the development of (ultra-) supercritical coal fired plants with a steam pressure as high as 33 MPa which are currently in operation worldwide (e.g. in Japan, Denmark, the United States…[4]). Using supercritical water would also result in a simpler construction as there is no more need for steam dryers or separators. The estimated efficiency varies between 42 and 45% depending on the details of the proposed system. Considering the large expertise currently available in supercritical water technology (such as steam turbines, high pressure steel alloys,

water purity control…) the SCWR looks to have some advantages compared to other GenIV designs. However, large material issues still need to be resolved, which are related to the interaction of corrosion and neutron damage of materials, as highlighted by Buongiorno and MacDonald [5]. As a first introduction of supercritical water, Vogt et al. [6] recently suggested a single-pass light water reactor design with supercritical water in the primary loop with a low exit temperature of about 380 °C. This would alleviate certain safety constraints the main SCWR designs have currently due to their much higher exit temperature (500°C).

Over the course of the past decades a number of core designs have finalized, including a Japanese design [7], a Korean design [8], a US design [5] and most recently a European design [9]. These designs differ considerably in fuel assemblies, flow layout and moderators which are used… Researcher continue to propose new core designs as shown by the work of Vogt et al. [6] and Reiss et al. [10]. The European design (HPLWR, High Performance Light Water Reactor) is remarkable having a three-pass core layout (Fig. 1A) combined with water rods for moderation. The system operates at 25 MPA, with an inlet and exit temperature of 280 °C and 500 °C. Between the passes mixing plena are used to reduce peak cladding temperatures.
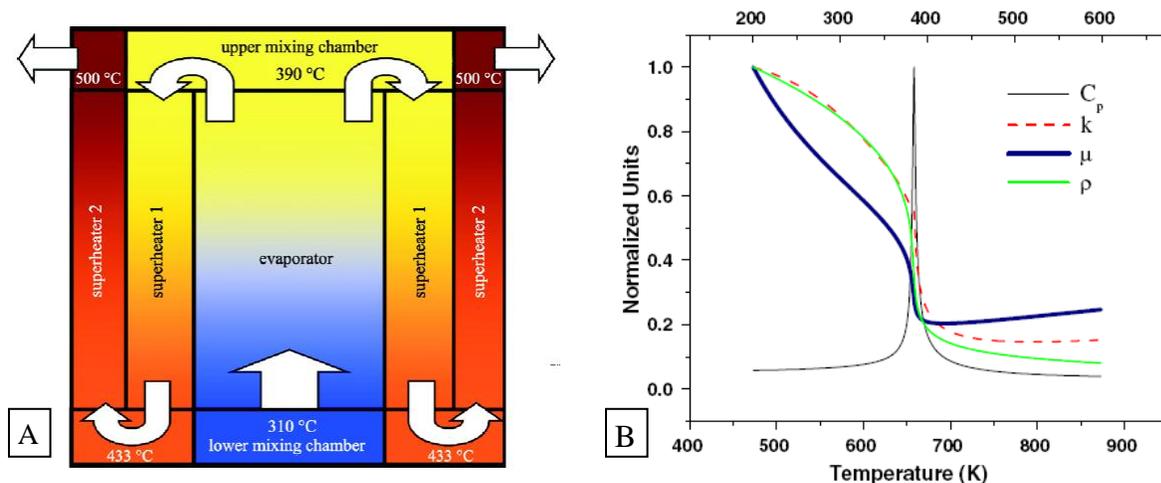

Figure 1. A: Three pass core arrangement proposed for the HPLWR (Fischer et al. [9]), B: normalized fluid properties (specific heat capacity Cp, thermal conductivity k, dynamic viscosity η and density ρ) for water at 25 MPa for a range of temperatures

As is well known, supercritical fluids experience strong changes in fluid properties. This is illustrated in Fig 1B. In the HPLWR core, the density varies between 780 kg/m³ and 90 kg/m³ with a sharp change near the pseudo critical point. This strong density difference could be used as the driving force for natural circulation, resulting in an inherently safer reactor without the need for large feed water pumps. Using natural circulation for improved safety of a nuclear system is not a novel idea, but it has not seen any commercial application except for residual heat removing. So far only one design, the ESBWR [11], has actually been constructed in a small size at Dodewaard, the Netherlands and was operated for decades. It should be noted that in the original SCWR designs, the once-through cycle is considered, whereby the steam passes through a turbine, becomes subcritical and then is repressurized with a pump. In order to achieve natural circulation this design needs to be modified into a 2 loop system (primary and secondary loop) which are interconnected by a heat exchanger.

Natural circulation loops however can become unstable under specific operational conditions (e.g. high power and low flow rate). Bouré et al. [12] presented a classification of the different types of instabilities. A static instability (flow excursion, the so called 'Ledinegg instability') can be described using only the steady state equations. In this case, a small change in the flow conditions will result in a new steady state not in the vicinity of the original one. For dynamic instabilities, such as the 'Density Wave Oscillations' (DWO), the steady equations are not sufficient to predict the behavior, or even the threshold of the instabilities. In such a situation, multiple competing solutions exist for the governing equations, and the system cannot settle down into anyone of them permanently. The system will move from one solution to the other, driven by a self-generated feedback. This feedback is due to the interaction of flow inertia and friction for the thermo-hydraulic modes. March-Leuba and Rey [13] presented a more detailed explanation of density wave oscillations. In a nuclear reactor another feedback mechanism appears: the neutronic feedback which couples the instant core section averaged fluid density to the power production through the moderation. This results in a more complex behavior, as shown by Yi et al. [14] for the US design of a SCWR.

The goal of this study is to examine the stability boundary of a naturally circulating HPLWR experimentally and numerically. To this end a setup has been designed and built, based on scaling analysis which will be briefly described further on. A code was also developed which performs a transient analysis of a perturbed steady state solution to determine if the system is stable or not. The code will be briefly described and validated before comparing the results of the experiments to the simulations.

1. Experimental facility: DeLight

1.1 Scaling the HPLWR

Studying the stability of a natural circulation driven HPLWR requires the design of a test facility. In order to reduce the pressure and temperature level and the power requirements imposed by the supercritical water to more suitable lab values, a scaling fluid was used. To design a scaled version of the HPLWR the governing equations (conservation of mass, momentum and energy and the equation of state) of the system should first be considered and made non-dimensional. Rohde et al. [15] describe the scaling procedure and derive a number of scaling factors based on the selected scaling fluid. After comparison of a large number of different fluids, Freon R23 (CHF_3) was selected as the scaling fluid based on the power requirement, the temperatures (the pseudo-critical temperature is only 33°C), the pressure (5.7 MPa) and safety (non flammable). The non-dimensional fluid properties agree well, with a maximum deviation of 8% for the density. Some relevant pseudo-critical fluid properties and scaling values are indicated in Table 1. Through linear stability analysis of a channel with supercritical water and of its scaled R23 counterpart, it was shown that the scaling rules result in the same stability behaviour, confirming the proposed scaling procedure and fluid selection (see Rohde et al. [15]).

Table I. Comparison of selected pseudocritical properties of H_2O and R23
and the resulting scaling rules, Rohde et al. [15]

	R23	H_2O	Scaling factor	
Pressure (MPa)	5.7	25	Length	0.191
Temperature (°C)	33.2	385	Diameter	1.06
Density (kg/m³)	537	317	Power	0.0788
Enthalpy (kJ/kg)	288	2153	Mass flux	0.74
Core inlet temperature (°C)	-21	280		
Core exit temperature (°C)	105	500		

1.2 DeLight facility

Based on the scaling rules an experimental facility has been constructed at the Delft university of Technology, named 'DeLight' (Delft Light water reactor facility). A schematic drawing is shown in Fig. 2. The loop is constructed of stainless steel tubing (6mm ID for the core sections, 10 mm ID for the riser and downcomer). The total height of the loop is 10 m. Up to 18 kW of heating (twice the nominal scaled power requirement) can be added in 4 tube sections (3 core sections and the moderator channel which mimics the water rod presence). Heating is done electrically (providing a uniform heat flux boundary) by sending a current through the tubes (up to 600A per core section using Delta SM15-200 power units). The power rating of each core section can be controlled individually, as the power distribution in the HPLWR is non uniform. The first core section or evaporator accounts for 53% of the power production, the second one (superheater I) for 30% and the final core section (superheater II) for 17%, see Fisher et al. [9]. Each core section is electrically insulated from the rest of the setup using a PEEK ring mounted in between two flanges. Valves are mounted between the core sections, at the inlet and exit of the core sections and at the exit of the riser. These can be used to introduce local friction values in the system, such as inlet systems or the plena mimicking actual reactor designs. It is well known that these local friction values can have a significant effect on the stability of a supercritical system, see e.g. Ambrosini and Sharabi [16].

To provide a stable pressure level, a buffer vessel is present at the top of the loop which has a moveable piston (Parker Series 5000 Piston Accumulator) connected to a nitrogen gas cylinder. By positioning this piston higher or lower the pressure level in the loop can be set at 5.7 MPa. Two heat exchangers (HX in Fig. 2) are mounted in series at the top section of the loop to extract the heating power and to set the inlet conditions. The first one uses cooling water (0.5 l/s) and cools R23 to 17°C. The second is an evaporator with R507a in which R23 is cooled down to a minimum temperature of -25°C. This temperature can be set by controlling the saturation pressure on the secondary side. Due to the differential thermal expansion of the core sections (wall temperatures can reach over 200 °C) and the other parts of the loop, the tubes are connected to the wall using moveable spacers which contain 2 pre-stressed springs. The bottom connection between the different core sections is made from a flexible tube of woven steel.

The loop contains a large number of sensors. At the top and bottom absolute pressure sensors are presents (p symbol in Fig. 2, ± 0.15%). Each valve is combined with a differential pressure drop sensor (Δp symbol in Fig. 2, ±0.5%, ±200/500 mbar) to measure the local pressure drop. The different core sections each contain 5 type K thermocouples to measure the local fluid temperature as it passes through the core section (T symbol in Fig. 2, ± 0.1K). These

thermocouples also have to be insulated electrically from the core to prevent the feed current passing through them. This was also done using PEEK rings. The individual thermocouple channels were calibrated carefully using 3 reference thermocouples which were calibrated over the entire temperature range by a certified body. As shown in Fig. 2 additional thermocouples are placed in the riser and downcomer section, as well as on the secondary side of the heat exchangers to monitor the heat removal. The R23 mass flow rate is measured using a coriolis meter (F symbol in Fig. 2, ± 0.25%, including a density measurement: ±0.005 kg/m³). Apart from the core sections the entire setup is insulated using Armacell$^{©}$ (25 mm thick) to reduce any heat loss/gain to/from the environment. A magnetic rotor pump is present in the loop, but a bypass can be set to allow for natural circulation, as shown in Fig. 2.
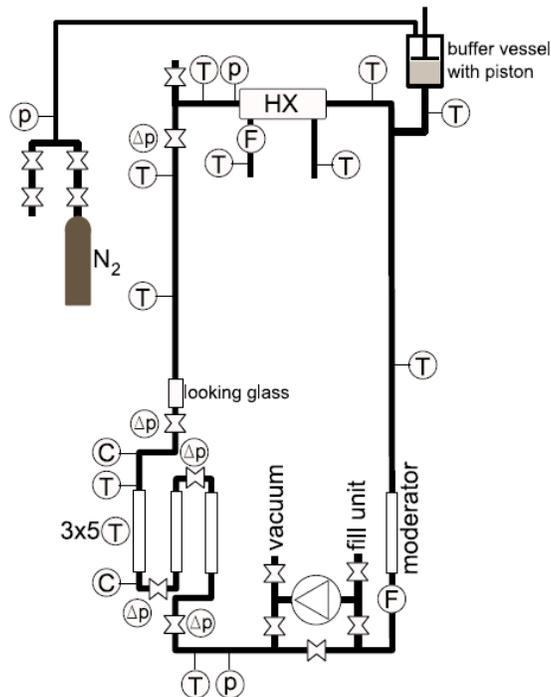

Figure 2. Schematic overview of the DeLight setup

The data acquisition system consists of a PC with one National Instruments PCI-6259 data acquisition card, connected to a National Instruments SCXI-1001 rack with two SCXI-1102B 32-channel amplifiers. This system is used for monitoring the experimental setup and for recording sensor signals. The measured and processed data are displayed on the PC screen which allows for continuous monitoring. Up to 64 multiplexed signals are recorded for further analysis. Additionally, seven signals (three temperature values, two pressure values, and the R23 and cooling water flow rates) are connected to a separate stand-alone data acquisition system with a National Instruments NI-6035 DAQ card. This system is used for safety monitoring and will shut down the power supplies if one of the signals exceeds prescribed limits.

The feedback of density perturbations on the reactivity $\mathcal{R}$ is implemented by measuring the average core density ρ with the help of the 15 installed thermo-couples and the equation of state for the density. These measured values are averaged over a sufficient time to determine the steady state value ρ_{ss}. Once the neutronic feedback is engaged, the measured density variations

are then used to calculate the reactivity via $\mathcal{R} = r_\rho(\rho(t) - \rho_{ss})$. The change in power due to the reactivity feedback is calculated with the help of a linearized six-group, point-kinetic model for the neutron density. The response of the heat flux to a power change is determined by using a first-order differential equation for the heat flux. The conduction in the fuel rod is in that case described by a single fuel time constant. The constants used for the reactivity feedback (density) are taken from a boiling water reactor, except for the constant r_α, which is obtained from [17]. The constants can be found in Table II.

Table II. Constants used for the reactivity feedback system in the Delight facility

Constant	Values
Fuel time constant τ_F	$2 - 6$ (s)
Neutron generation time Λ	5.10^{-5} (s)
Precursor decay constants λ_i	0.0127,0.0317,0.115,0.311,1.4,3.87
Delayed neutron fractions β_i (normalized)	0.038,0.213,0.188,0.407,0.128,0.026
Total delayed neutron fraction β	0.0065
Reactivity constant r_ρ	$3.526.10^{-5}$ (m^{3}kg^{-1})

1.3   Experimental procedure

To experimentally determine the stability behaviour of the setup, the following procedure was used. First, the pump was used to start the circulation of the Freon in the loop and a small amount of heating was added (1 kW). The pump was then switched off and bypassed, resulting in a naturally circulating fluid. The pressure was then raised about the critical pressure and the cooling setup was turned on. By simultaneously controlling the position of the piston and slowly incrementing the added heat, the system was brought to the required testing conditions (5.7 MPa, and a specified power input in the HPLWR distribution). Once a steady state situation has been reached (judged by the absolute pressure variations of about 0.25 bar), the measurement was started. First over a period of 2 minutes the average core density is recorded. Then the neutronic feedback would be switched on, calculating the power correction based on the measured value average density. If the system is unstable, the neutronic feedback will make the power input fluctuate with a growing amplitude. These signals would then be recorded until power saturation is reached. The saturation value was set to 10% of the power input to prevent large pressure fluctuations in the loop. If the system was stable, and no oscillations were present two minutes after switching on the feedback, a step increase in the power (250 or 500W) was done for 5 seconds. The decaying signal was then recorded until it was no longer distinguishable. The instabilities could be seen in all the recorded signals but they were most apparent in the temperature signals (e.g. at the inlet of the riser). Two examples of measured temperature signal are shown in Fig. 3

These signals were then processed using signal analysis tools. All the sensor signals are sampled with a frequency of f_s=120 Hz and then resampled to f_r=20 Hz. Before resampling, the signals are filtered with a cut-off frequency of 9Hz (Nyquist theorem). This was done using a digital filter implemented in Matlab. The resampling is done by averaging each 6 samples. These resampled data were then used to determine the decay ratio 'DR'. This was done by fitting the

equation $y = (1 - c - a) \cdot e^{b_1 \cdot t} + c + a \cdot e^{b_2 \cdot t} \cdot \cos(\omega \cdot t)$ to the first two periods of the auto correlation function (ACF) of the signal. The DR is then defined by equation (1). These equations have been previously derived by Marcel [18] for a natural circulation boiling water reactor. The DR uncertainty can be estimated through standard error analysis procedures and was found to be less than 5%. As an extra check for the resonance frequency ω, the auto power spectral density is also determined, verifying it contains a single well defined peak at that frequency.

$$DR = e^{\frac{2 \cdot \pi \cdot b_2}{|\omega|}}$$
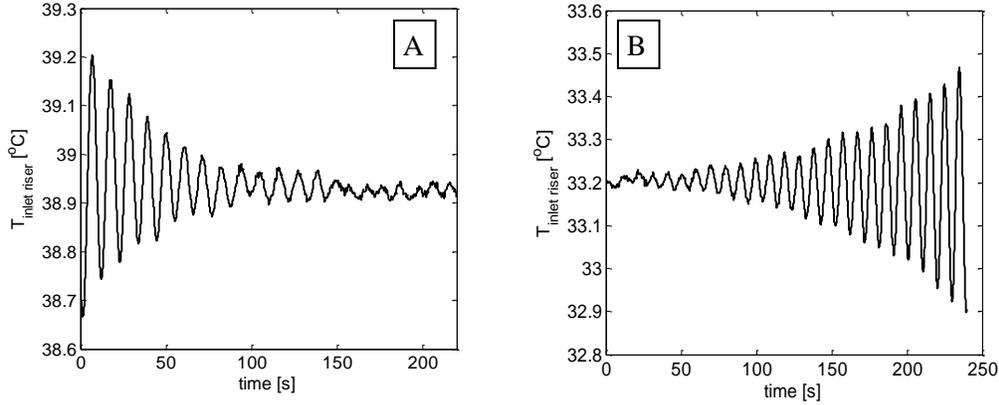(1)

Figure 3. Examples of a stable (A) and unstable (B) temperature signal
measured at the inlet of the riser section

2.   Numerical simulations

Different numerical methods exist to determine the stability a natural circulation system. The system can be described through a set of non-linear coupled differential equations, which are then solved to determine the steady state solution. Based on this solution the stability of the system can be determined by either performing transient simulations [19], Laplace transformation [20] or eigenvalue analysis of the linearized set of equations [21]. As an alternative system codes have been used ([16]) or even CFD analysis of 3D flow ([22]).

2.1   Description of the code

For one dimensional channel flow, the time dependent mass, momentum and energy conservation equations can be written as follows using M (mass flow rate), p (pressure) and h (enthalpy). A represents the tube surface area (variable), f the friction factor (Haaland relationship), g the gravimetric acceleration and q' the linear heating rate. The dynamic viscosity was defined using a series of splines based on NIST property data [23]. To close the system of equations, an equation of state $\rho = \rho(p,T)$ is needed. A first order Taylor expansion of the density in terms of temperature and pressure was used (Eq. (5)) to calculate the change in density:

$$A \frac{\partial \rho}{\partial t} + \frac{\partial M}{\partial x} = 0$$
(2)

$$\frac{\partial \mathbf{M}}{\partial t} + \frac{\partial}{\partial x}\left(\frac{\mathbf{M}^2}{A\rho}\right) = -A\frac{\partial p}{\partial x} - f\frac{P_{wall}\mathbf{M}^2}{8A^2\rho} - K_i\frac{M^2}{2A\rho}\delta(x - x_i) + \rho g A \tag{3}$$

$$A\frac{\partial \rho \mathbf{h}}{\partial t} + \frac{\partial \mathbf{M}\mathbf{h}}{\partial x} = q' + A\frac{\partial p}{\partial t} \tag{4}$$

$$d\rho = \left[\frac{\partial \rho}{\partial T}\right]_P dT + \left[\frac{\partial \rho}{\partial p}\right]_T dp \tag{5}$$
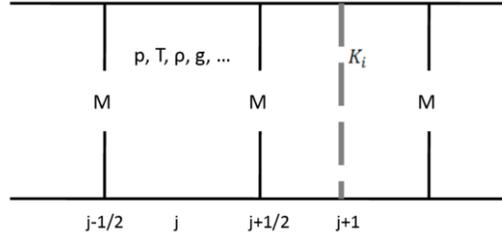

Figure 4. Discretization grid.

The equations for the conservation of mass, momentum and energy are discretized using a first order implicit upwind scheme. All physical quantities are defined on the nodes, apart from the mass flow rate, as illustrated in Fig. 4. The pressure in the loop P_{sys} is imposed at the top of the downcomer. As the system heats up, but has a constant volume, some mass needs to leave the system. This outflow of mass is done in the nodes after the heat exchanger and before the top of the downcomer. It is determined with a proportionality constant F ($6\ 10^{-5}$) and the local pressure p_j (Eq. (6)). A pressure correction method for compressible flow (Bijl, [24]) is employed.

$$M_{out} = F\left(p_j - P_{sys}\right) \tag{6}$$

Each discretized conservation equation forms a linear system of equations with size N (number of nodes) and can be written in a matrix form. This matrix is cyclic and tri-diagonal due to the choice of the upwind scheme and the loop configuration. The system of equations can then be solved with the Sherman-Morrison method as described by Press et al. [25]. The solution algorithm will be iterated until convergence is reached. The convergence criterion is satisfied when the new iterated value for the pressure p^{k+1} is within a specified limit (0.1%) of the previous iteration value p^k, everywhere in the system.

The program starts with the coolant at a constant temperature throughout the loop and at rest. At this moment no heat is added or extracted from the system. The linear heat rate, q', in the core sections and in the heat exchanger gradually rises to the desired level at a specified rate during the warm-up period. After this warm-up period, the program is run long enough for a steady state solution to be reached. When a steady state solution has been reached, the average core coolant density is determined and with the point-kinetic equations (Duderstadt and Hamilton [26]), steady state values for the neutron- and precursor densities are found. In the next time step, a neutronic feedback mechanism is turned on. If the coolant density coefficient of reactivity is r_ρ, any deviation in the average coolant density in the core, $\delta\rho$, results in an

insertion of reactivity: $\mathcal{R} = r_\rho . \delta\rho$. This extra reactivity is used in the point-kinetic equations to calculate a new value for the neutron density, resulting in a new value for the power P, since it is directly proportional to the neutron density (Eq. (7)).

$$P = V w_f \Sigma_f n(t) v_n \tag{7}$$

With V the volume of the fuel, w_f the energy released per fission, Σ_f the macroscopic cross-section of a fission event and v_n the velocity of a neutron. The volume cancels out in the equations, the other constants were determined from the work of Ortega-Gómez et al. [21]. In practice the change in linear heat rate will not be instantaneous, since it takes some time to transport heat from the fuel elements to the coolant. It is assumed that this heat-transfer function can be described by a first order power transfer function: the increase in linear heat rate, $q'_{extra}(t)$ at time t, in reaction to a step change in power $P_{extra}(t_0)$ at time t_0, can be described by Eq. (8). The constant c characterizes the time it takes to fully transfer the extra heat from the fuel into the coolant. Initially c is set to 1 [1/s] as a default value.

$$q'_{extra}(t) = \frac{P_{extra}(t_0)}{L_{heated}} \left[1 - e^{-c(t-t_0)} \right] \tag{8}$$

To study the stability of the system, the steady state solution is perturbed by a small increase in power (default value is 0.02 kW) during one time step, which results in a slightly increased linear heat rate during that time step. The subsequent dynamic behaviour of the mass flow rate at the core inlet is determined from which the DR can be derived.

2.2   Validation of the code

As a validation the loop studied by Jain and Uddin [19] was studied, and the power vs. flow data was reproduced. The results are shown in Fig. 5. As can be seen, the agreement is very good. A thorough grid size and time step dependency study was performed. This was done for the DeLight model (thus using supercritical R23 at 5.7 MPa) for a power of 5 kW and an inlet temperature of 0°C. The results are presented in Figure 5B. In this graph the ratio of the predicted mass flow rate to that predicted by the finest grid size or time step considered is shown for various time steps (blue line) and various grid sizes (red line). For the varying time step simulations the grid size was fixed at 2 cm, for the varying grid size simulations the time step was fixed at 0.1s. The results show a straightforward converging behaviour for the time step but a more varying behaviour for the grid size. As a result, a grid size of 1 cm and a time step of 0.1s was selected for the simulations. It was verified that the predicted DR trend, in particular the crossover from stable to instable was also independent of the grid size and time step used.

3.   Results and discussion

To present the measured and simulated stability data, two non dimensional numbers will be used. These are the subcooling number N_{SUB} (Eq. (9)) and the phase change number N_{PCH} (Eq. (10)). These numbers have been derived in the stability scaling analysis by Rohde et al. [15], and use the pseudocritical point as a reference condition (h_{pc} for R23 at 5.7 MPa = 288.03 kJ/kg). Ambrosini and Sharabi [16] previously derived similar non dimensional numbers as an extension to earlier work done in boiling channels.
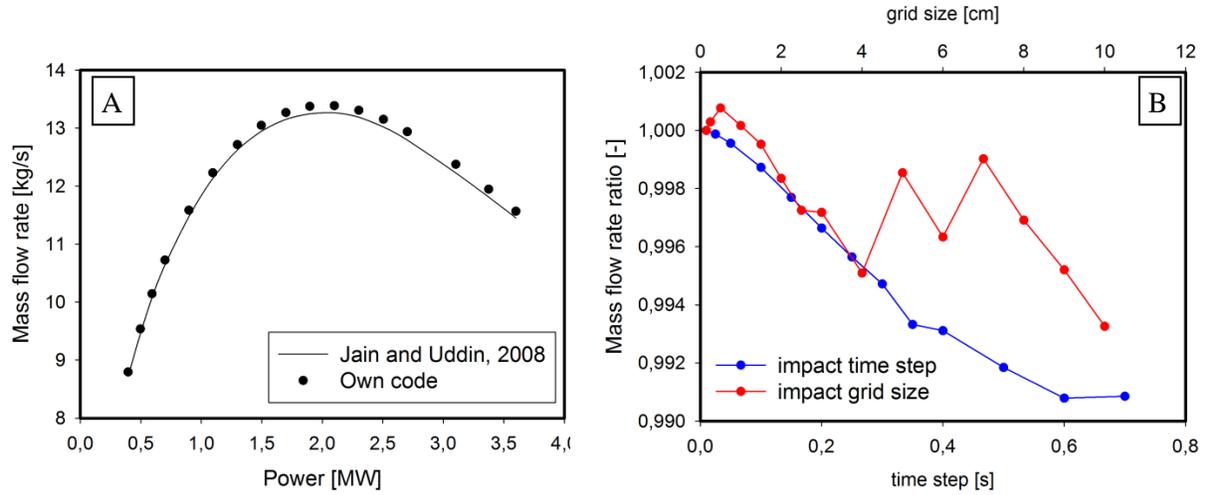
Figure 5: A: comparison of the simulated power-flow to data by Jain and Uddin [19], B: grid and time step independence study for DeLight model (5kW, T_{in}: 0°C)

$$N_{SUB} = \frac{h_{pc} - h_{in}}{h_{pc}} \tag{9}$$

$$N_{PCH} = \frac{P}{M \cdot h_{pc}} \tag{10}$$

Figure 6 shows the experimentally determined DR values for the DeLight setup with a fuel time constant of 6 seconds. This is typical value for nuclear reactors. This plot is derived from the available experimental data through a third order fitting procedure. This was done in order to better visualise the stability behaviour in the entire plane, rather than judging it from scattered data points. During the experiments the inlet temperature is kept constant, and the DR is measured for different power levels. The power step to the next point varied, and was kept small near to the transition boundary. The areas in deep purple (left top corner, right bottom area) are zones where no data is available. This is because the DR was either
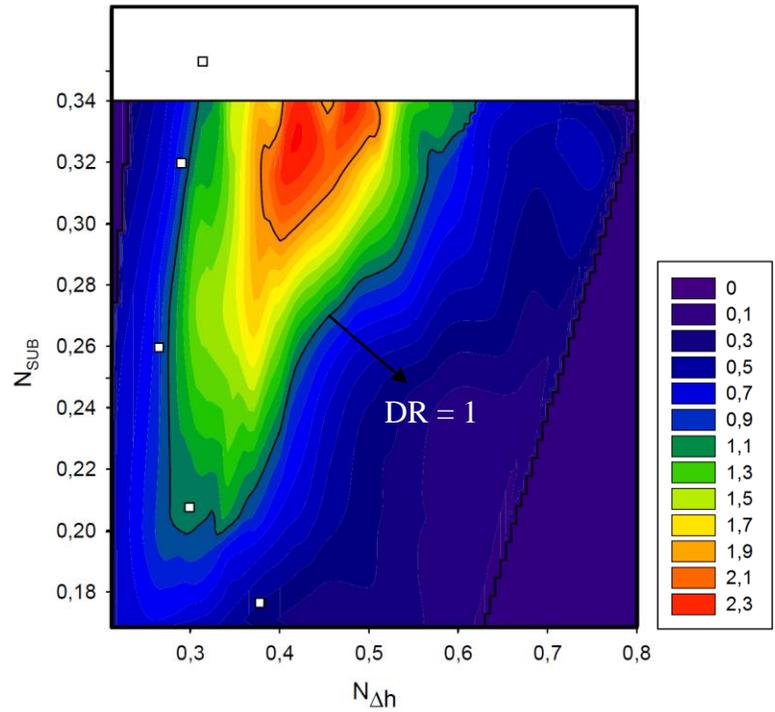

Figure 6: Comparison of experimentally determined DR values and the numerically predicted stability boundary

too small to measure (left top bottom) or the power limit was reached (right bottom area). The setup is also limited when it comes to inlet temperatures, and the maximum N_{SUB} value is 0.34. The stability boundary (DR = 1) is indicated in the graph. As can be seen there is a definite unstable zone which increases in intensity as the inlet temperature decreases.

The white symbols in Fig. 6 indicate the numerically predicted stability boundary. The points shown on the graphs are determined through linear interpolation between two N_{PCH} values respectively with a DR smaller and larger than 1 for a given inlet temperature. As can be seen the agreement between the left boundary of the unstable zone and the numerically predicted points is very good, especially for high N_{SUB} values. At low N_{SUB} values, the code seems to underestimate stability, indicating a cross-over point where the experiments showed only stable operating conditions. It is unclear what is the cause; it could be due to the small differences in the numerical and experimental implementation of the neutronic feedback or the presence of a small preheating section in the downcomer to better control the inlet temperature which is not considered in the code. The code will be modified to consider both these scenarios to see if either can explain the difference. Also, so far mainly low powers have been studied in the code. An initial scan at higher powers for a single inlet temperature indicated that a second transition was found as well, however at much higher $N_{\Delta h}$. This could again be due to the aforementioned reasons and will be studied in more detail.

The impact of three parameters was studied experimentally. Lowering the fuel time constant was found to stabilise the system, reducing the size of the instable area, shifting it up to the left top corner. Increasing the inlet friction resulted in a more stable system, lowering the DR values. The most prominent effect was found for the power distribution: changing the distribution to a uniform case (each core gives the same amount of power) made the system significantly more stable, shifting the unstable area to much higher N_{PCH} values (~ 0.65).

4. Conclusions

This paper presents the preliminary results of an experimental and numerical study on the stability of a naturally circulating HPLWR. The experiments (through a scaled loop using R23) revealed a clear instable area in the stability plane. The simulations were able to capture the left boundary with a good accuracy for high NSUB values, but showed some deviation at smaller values. A parameter study was performed experimentally, finding that lowering the fuel time constant and increasing the inlet friction resulted in a more stable system. Interestingly changing the power distribution from HPLWR (53 – 30 – 17%) to uniform, made the system considerably more stable as well.

5. Acknowledgements

6. References

[1].   OECD/IEA, 2008. World Energy Outlook 2008: Presentation to the Press. London, UK.

[2].   Euratom (European Commission, Directorate General for Research Euratom), 2007. The Sustainable Nuclear Energy Technology Platform, A Vision Report. European Commission, Brussels, Belgium.

[3].   GIF, 2002. A Technology Roadmap for Generation IV Nuclear Energy Systems. Generation IV International Forum, GIF-002-00.

[4].   M.R. Susta, "Supercritical and Ultra-Supercritical Power Plants – SEA's Vision or Reality", Proceedings of POWERGEN ASIA 2004, 2004, pp. 1-23.

[5].   J. Buongiorno, P.E. MacDonald, "Supercritical water reactor (SCWR), progress report for the FY-O3 Generation IV R&D activities for the development of the SCWR in the U.S"., Report INEEL/EXT-03-01210, 38 pages, 2003.

[6].   B. Vogt, K. Fischer, J. Starflinger, E. Laurien, T. Schulenberg, "Concept of a pressurized water reactor cooled with supercritical water in the primary loop", Nuclear Engineering and Design, Vol. 240, 2010, pp. 2789-2799.

[7].   Y. Oka, S.I. Koshizuka, "Concept and Design of a Supercritical-Pressure, Direct-Cycle Light-Water Reactor", Nuclear Technology, Vol. 103, 1993, pp. 295-302.

[8].   Y.Y. Bae, J. Jang, H.Y. Kim, H.Y. Yoon, H.O. Kang, K.M. Bae, "Research activities on a supercritical water reactor in Korea", Nuclear Engineering and Technology, Vol. 39, 2007, pp. 273-286.

[9].   K. Fischer, T. Schulenberg, E. Laurien, " Design of a supercritical water-cooled reactor with a three-pass core arrangement", Nuclear Engineering and Design, Vol. 239, 2009, pp. 800-812

[10].   T. Reiss, G. Csom, S. Feher, S.Czifrus, "The simplified supercritical water cooled reactor, SSCWR, a new SCWR design", Progress in Nuclear Energy, Vol. 52, 2010, pp. 177-189

[11].   C.P. Marcel, M. Rohde, T.H.J.J. Van der Hagen, "Experimental investigations on the ESBWR stability performance", Nuclear Technology, Vol. 25, 2008, pp. 232-244

[12].   J.A. Bouré, A.E. Bergles, T.S. Tong, " Review of two-phase flow instability", Nuclear Engineering and Design, Vol. 25, 1973, pp. 165-192

[13].   J. March-Leuba, J.M. Rey, "Coupled thermohydraulic-neutronic instabilities in boiling water nuclear reactors: a review of the state of the art", Nuclear Engineering and Design, Vol. 145, 1993, pp. 97-111

[14].   T.T. Yi, S. Koschizuka, Y. Oka, "A linear stability analysis of supercritical water reactors (II): coupled neutronic thermal-hydraulic instability", Journal of Nuclear Science and Technology, Vol. 41, 2004, pp. 1176-1186

[15].   M. Rohde, C.P. Marcel, C. T'Joen, A. Class, T.H.J.J. Van der Hagen, T.H.J.J., "Downscaling a supercritical water loop for experimental studies on system stability", International Journal of Heat and Mass Transfer, Vol. 54, 2011, pp. 65-74

[16].   W. Ambrosini, M. Sharabi, "Dimensionless parameters in stability analysis of heated channels with fluids at supercritical pressures", Nuclear Engineering and Design, Vol. 238, 2008, pp. 1917-1929

[17].   Schlagenhaufer, M., Vogt, B., Schulenberg, T., "Reactivity control mechanisms for a HPLWR fuel assembly", Proceedings of Global 2007, Boise, Idaho, September 9-13 2007

[18].   Marcel, C.P., "Experimental and Numerical Stability Investigations on natural Circulation Boiling Water Reactors", Ph.D. Thesis, 2007, Delft University of Technology

[19].   P.K. Jain, R. Uddin, "Numerical analysis of supercritical flow instabilities in a natural circulation loop', Nuclear Engineering and Design, Vol. 238, 2008, pp. 1947-1957.

[20].   D.D.B. Van Bragt, T.H.J.J. Van der Hagen, "Stability of natural circulation boiling water reactors: Part II – parametric study of coupled neutronic-thermohydraulic stability", Nuclear Technology, Vol. 121, 1998, pp. 52-62

[21].   T. Ortega Gómez, A. Class, R.L. Lahey Jr., T. Schulenberg, "Stability analysis of a uniformly heated channel with supercritical water", Nuclear Engineering and Design, Vol. 238, 2008, pp. 1930-1939

[22]. Sharabi, M.B., Ambrosini, W., He, S., "Prediction of unstable behaviour in a heated channel with water at supercritical pressure by CFD models", Annals of Nuclear Technology, Vol. 35, 2008, pp. 767-782

[23]. M.L. Huber, E.W. Lemmon, M.O. McLinden, "NIST Reference fluid thermodynamic and transport properties", REFPROP: U.S. Department of Commerce, Technology Administration, 2002, version 7.0

[24]. H. Bijl, "Computation of flow at all speeds with a staggered scheme", PhD thesis, Delft University of Technology, 1999

[25]. W.H. Press, S.A. Teukolsky, W.T. Vetterling, B.P. Flannery, "Numerical recipes in C: the art of scientific computing": Cambridge University Press, 1992

[26]. J.J. Duderstadt, L.J. Hamilton, "Nuclear reactor analysis", John Wiley & Sons, 1976